

1
2
3
4
5
6
7
8
9
10
11
12
13
14
15
16
17
18
19
20
21
22
23
24
25
26
27
28
29
30
31
32
33

International Journal of Food Microbiology, Volume 154, Issue 3, 15 March 2012, Pages 169-176

Growth curve prediction from Optical Density Data

I Mytilinaios, M. Salih, H.K. Schofield and R.J.W. Lambert

¹Applied Microbiology Group,
Cranfield Health
Cranfield University
Cranfield MK43 0AL, U.K.

May, 2011

Key Terms: Baranyi, Gompertz, logistic, predictive modelling

Abstract

34

35

36

37 A fundamental aspect of predictive microbiology is the shape of the microbial growth curve and
38 many models are used to fit microbial count data, the modified Gompertz and Baranyi equation
39 being two of the most widely used. Rapid, automated methods such as turbidimetry have been
40 widely used to obtain growth parameters, but do not directly give the microbial growth curve.

41 Optical density (OD) data can be used to obtain the specific growth rate and if used in conjunction
42 with the known initial inocula, the maximum population data and knowledge of the microbial
43 number at a predefined OD at a known time then all the information required for the reconstruction
44 of a standard growth curve can be obtained.

45 Using multiple initial inocula the times to detection (TTD) at a given standard OD were obtained
46 from which the specific growth rate was calculated. The modified logistic, modified Gompertz, 3-
47 phase linear, Baranyi and the classical logistic model (with or without lag) were fitted to the TTD
48 data. In all cases the modified logistic and modified Gompertz failed to reproduce the observed
49 linear plots of the log initial inocula against TTD using the known parameters (initial inoculum, MPD
50 and growth rate). The 3 phase linear model (3PLM), Baranyi and classical logistic models fitted the
51 observed data and were able to reproduce elements of the OD incubation-time curves. Using a
52 calibration curve relating OD and microbial numbers, the Baranyi equation was able to reproduce
53 OD data obtained for *Listeria monocytogenes* at 37 and 30°C as well as data on the effect of pH
54 (range 7.05 to 3.46) at 30°C.

55 The Baranyi model was found to be the most capable primary model of those examined (in the
56 absence of lag it defaults to the classic logistic model). The results suggested that the *modified*
57 logistic and the *modified* Gompertz models should not be used as Primary models for TTD data as
58 they cannot reproduce the observed data.

59

60 **1 Introduction:**

61 A fundamental aspect of predictive microbiology is the shape of the microbial growth curve.
62 General population growth can be modelled using the logistic model and variations of this model
63 have been used in many diverse areas such as the analysis of fish stocks, forestry management
64 and human population growth (e.g. [Alexandrov 2008](#)). The general pattern of growth is sigmoidal,
65 with an apparent slow phase followed by a more rapid increase in numbers followed by a slowing
66 down, finally reaching a maximum population level. In most texts it is noted that the growth of
67 bacteria also follows a similar pattern: a lag before replication, followed by exponential growth and
68 then a period of maximum population density eventually followed by the 'death-phase'. A major
69 difference is that the microbial growth curve is depicted in terms of log numbers of microbes. The
70 microbial growth curve (as log numbers) has the characteristic sigmoid shape and the varieties of
71 models which are used to fit the curve reflect this sigmoid character. There are two principal
72 *empirical* curves used – the symmetric modified logistic and the asymmetric modified Gompertz
73 ('modified' by virtue of using log numbers rather than numbers explicitly). Many models in the
74 microbiological literature are variations on these two themes ([Li et al., 2007](#); [Pruitt and Kamau](#)
75 [1993](#); [Zwietering et al. 1990](#)).

76
77 The Baranyi model, however, is different to the normal growth models in that it is based on the
78 logistic model of growth, but has an additional function which deals with the presence of lag
79 making it a non-autonomous differential equation ([Baranyi et al., 1993, 1993b](#); [Baranyi and](#)
80 [Roberts 1994](#));

81
$$\frac{dn}{dt} = \alpha(t)\mu(n)n$$

82 Where $\mu(n)$ is a function of the specific growth rate, n is the numbers of microbes and $\alpha(t)$ is
83 termed the adjustment function. The derived equation uses the idea of Michaelis –Menten kinetics
84 to suggest a lag time during which organisms adapt from one environment (the culture) to the test
85 environment. The function used essentially delays the time before growth occurs.

86
87 [Baranyi and Roberts \(1995\)](#) in their paper on the fundamentals of mathematics in predictive
88 microbiology stated that rapid methods such as turbidimetry or conductimetry cannot be used
89 directly to obtain growth parameters such as the specific growth rate if the rescaling function
90 employed has a constant other than zero;

91 “if the measured quantity is q , then $q = f(x)$, where f is a linear calibration function: $f(x) = a \cdot x + b$. If
92 b is different from 0 then neither q nor $\log q$ is linearly proportional to $\log x$. Hence, in a strict
93 sense, the rate of change in q should not be used to estimate the viable count specific growth rate
94 unless the proportionality of q (turbidity, conductance, etc.) to the original cell concentration, x , has
95 been established over the complete matrix of environmental variables (temperature, pH, a_w). Nor
96 should the viable count models describing $x(t)$ be directly applied to model $q(t)$. New calibration
97 function, or other considerations, should be taken into account to model $q(t)$ and/or to compare it
98 with the viable count model.” (Baranyi and Roberts 1995).

99
100 Models used to examine the shape of microbial growth generally require four parameters: the initial
101 and final population levels (I_0 and MPD respectively), the maximum specific growth rate and the
102 time at which this occurred. If three pieces of information are available, e.g. the initial population,
103 the MPD and the specific growth rate, then knowledge of the population at a specific time can be
104 used to reproduce the growth curve simply by substituting the values into the equations and
105 solving for the missing parameter. Herein we show that this seemingly simple hypothesis serves as
106 a “consideration” and also has ramifications on the validity of the modified empirical growth curves,
107 whilst adding value to the interpretation of the Baranyi equation.

108

109 **2 Methods: Microbes and Models**

110 **2.1 MICROBES**

111 From a previously prepared and stored slope on tryptone soya (TSA) of the pure culture of *L.*
112 *monocytogenes* (Lm 252 an industrial isolate donated by Nestlé), a portion was removed with a
113 sterile loop, transferred into a conical flask containing 80 ml tryptone soya broth (TSB) and
114 incubated with shaking (150 rpm) at 30°C overnight. The resulting culture was split into four
115 portions and centrifuged at 500g for 10 minutes. Two of the resulting pellets were resuspended in
116 TSB (2 ml) and pooled. The resuspended culture (1ml) was transfer into TSB (9ml) in a universal
117 tube and mixed thoroughly; 1ml of this suspension was diluted in TSB to obtain a standard optical
118 density of approximately 0.5 with a 1cm path length at 600nm (M350 Double Beam U.V. Visible
119 Spectrometer). From the standardised culture a series of decimal dilutions were prepared in TSB
120 (labelled 0 to -9).

121 **2.2 PREPARATION OF MICRO-ARRAY PLATES**

122 The Bioscreen micro-array plates were filled as follows: all wells except column 10 received 200µl
123 of TSB. The wells of column 10 received 400µl of the appropriate serial dilutions (with the highest
124 inoculum (the zero dilution) in well 100. Using a multi-pipette, 200µl were removed from each well
125 of column 10 and transferred into the wells of column 9, the -1 dilution, mixed by repeated
126 syringing, etc. This was repeated across the plate discarding the excess 200µl after final mixing.
127 Theoretically for an initial inoculum of 1×10^9 cfu/ml, this method will give a range from $9 \log_{10}$ to -
128 $2.7 \log_{10}$ cfu/ml. The OD of a sample in the Bioscreen is dependent on the volume used: a
129 standard OD of 0.5 measured in the spectrophotometer has an OD of 0.29 at 600nm for a volume
130 of 200µl in the Bioscreen.

131 Plates were typically incubated for 1 to 3 days, with the optical density of the wells being read at
132 600nm every ten minutes.

133

134 **2.3 EFFECT OF PH**

135 A range of 30 different pH in TSB (pH 7.05 to 3.46 adjusted with filter sterilised HCl (0.01M) in
136 approx. 0.35 pH unit intervals) each with 3 replicates per plate and done in duplicate on separate
137 machines were tested against a single inoculum size of *L. monocytogenes* (LM 252) at 30°C.

138

139 2.4 MODELS AND DATA ANALYSIS

140

141 From the resulting Bioscreen OD/time data, the background OD due to the media was removed
 142 from each. A time to detection (TTD) criterion of OD = 0.2 was then used on the background
 143 corrected data: TTD were found using linear interpolation between OD/time values which straddled
 144 the OD = 0.2 value. For a given set of environmental conditions a plot of the log of the initial
 145 inoculum size against the time to detection (TTD) gives a straight line relationship with gradient
 146 equal to the reciprocal of the specific growth rate ([Cuppers and Smelt 1993](#)). In the absence of a
 147 lag the line will intersect the log initial inoculum axis at the detection value for the given OD
 148 criterion used.

149

150 TTD data have approximately constant variance until the initial inoculum level is less than 10^2
 151 cfu/ml, below this level the variance increases ([Bidlas et al. 2008](#)). To preclude the need for
 152 weighted regression or for a data transformation data below this inoculum size threshold were
 153 censored in the regression fits.

154

155 2.4.1 Modified logistic and Gompertz

156 The re-parameterised modified logistic and Gompertz models ([Zwietering et al. 1990](#)) were
 157 rearranged to equate the initial log inoculum with the time to detection of a known number of
 158 microbes per ml (N_D), giving equations 1 and 2 respectively.

159

$$160 \quad t_D = \lambda - \frac{A}{4\mu_m} \left\{ \ln \left[\frac{A}{\log N_D - \log N_0} - 1 \right] - 2 \right\} \quad (\text{Eq.1, modified logistic})$$

161

$$162 \quad t_D = \lambda - \frac{1}{\mu_m} \left(\frac{A}{e} \right) \left[\ln \left\{ \ln \left(\frac{A}{\log N_D - \log N_0} \right) \right\} - 1 \right] \quad (\text{Eq.2, modified Gompertz})$$

163

164 2.4.2 Three phase linear Model (3PLM)

165 The 3-phase linear model is a simplified model of the growth curve. Its simplicity has been
 166 regarded by some as its strength and too simplistic by others ([Baranyi 1997](#); [Buchanan et al. 1997](#);
 167 [Garthright 1997](#)). The 3-phases are given by the following;

$$168 \quad \log N = \log N_0 \text{ if } t \leq t_\lambda \text{ else}$$

$$169 \quad \log N = \log N_0 + \mu(t - t_\lambda) \text{ if } t: t_\lambda \leq t < t_{\max} \text{ else}$$

$$170 \quad \log N = \log N_{\max}, \text{ when } t \geq t_{\max}$$

171 The parameter t_λ is the duration of lag time. This equation can be rearranged to equate the initial
 172 log inoculum with the time to detection of a known number of microbes per ml (N_D),

$$173 \quad t_D = \lambda + \frac{\log N_D - \log N_0}{\mu_m} \quad (\text{Eq.3})$$

174 2.4.3 Baranyi and logistic models

$$\log N = \log N_0 + \frac{y_1}{\ln(10)} - \frac{y_2}{\ln(10)}, \quad \text{where}$$

$$175 \quad y_1 = \mu_m t + \ln \left[e^{-\mu_m t} - e^{-\mu_m (t+t_{\text{lag}})} + e^{-\mu_m t_{\text{lag}}} \right] \quad \text{and}$$

$$176 \quad y_2 = \ln \left[1 + 10^{(\log_{10} N_0 - \log_{10} M)} \left(e^{\mu_m (t-t_{\text{lag}})} - e^{-\mu_m t_{\text{lag}}} \right) \right] \quad (\text{Eq.4})$$

177 The Baranyi model, which is a non-autonomous equation, cannot be rearranged to obtain time
 178 explicitly. In the absence of lag the Baranyi model defaults to the basic logistic model of growth in
 179 which the time to detection for a given number of microbes is given by

$$180 \quad t_D = \frac{1}{\mu} \ln \left\{ \frac{\frac{M}{N_0} - 1}{\frac{M}{N_D} - 1} \right\} \quad (\text{Eq. 5a})$$

181 Where M = maximum population density (cfu/ml), N_D = numbers of microbes per ml at the
 182 detection value, N_0 = initial inoculum level (cfu/ml) , μ = specific growth rate. In general $N_0 \leq N_D$
 183 $< M$. When $N_0 = N_D$, $t_D = 0$.

184 A simple, empirical, approximation to the Baranyi equation when a lag exists is given by

185 $t_D = \lambda + \frac{1}{\mu} \ln \left\{ \frac{\frac{M}{N_0} - 1}{\frac{M}{N_D} - 1} \right\}$

186 (Eq. 5b)

187 3 Results

188

189 3.1 GROWTH RATE OF *L. MONOCYTOGENES* AT 37°C FROM OD DATA

190 The optical density/incubation time curves for different initial inocula of *Listeria monocytogenes* in
191 TSB are shown in [Figure 1](#). Each individual curve was essentially congruent with all other curves:
192 there is no decrease in the slope with decreasing initial inocula. The average maximum OD
193 reached was 0.99 ($\sigma = 0.034$, se. mean = 0.004). For each curve, the TTD of OD = 0.2 was found
194 using simple linear interpolation between OD/time data which straddled the OD = 0.2 position. The
195 analysis of the TTD of these multiple dilutions of initial inocula (the zero dilution starting culture had
196 a viable count of 1.11×10^9 cfu/ml), showed a simple linear relationship between the initial inoculum
197 and the TTD criterion used ([Figure 2](#)). The reciprocal of the gradient gives a growth rate of 0.0092
198 \log_{10} cfu/ml/min, which equates to a specific growth rate of 1.27 ln cfu/ml/h ([Table 1](#)). The intercept
199 of 961 minutes corresponds to the theoretical time taken for a single organism per ml to reach the
200 TTD= 0.2 criterion; when TTD = 0, the regression line cuts the axis at an initial log inoculum of 8.81
201 \log_{10} cfu/ml (95% CI 8.77-8.86), which was statistically equivalent to the \log_{10} cfu/ml count of the
202 viable count recorded from multiple wells with OD = 0.2. Hence in this case there was no
203 measurable lag; this was also confirmed from an analysis of Figure 1 – the highest inocula
204 examined do not show any lag period.

205

206 3.2 FITTING THE MODIFIED LOGISTIC AND GOMPERTZ MODELS TO OD DATA

207 From a plate count the MPD of the *Listeria monocytogenes* culture was 9.8 \log_{10} cfu/ml, the initial
208 inoculum size for each well was calculated from the plate count of the initial inoculum and the
209 dilution sequence used. From the OD data, the specific growth rate and lag were obtained, hence
210 all the parameters required to reproduce the growth curve using either the modified logistic or
211 Gompertz equations were present. Equations 1 and 2 were used to calculate the TTD for the given
212 initial inocula using the observed parameters. A plot of the calculated TTD (TTD_{calc}) against the
213 initial inocula gave a regression fit of $TTD_{calc} = -125.53 \log N_0 + 1087.7$, $r^2 = 0.999$ and $TTD_{calc} = -$
214 $144.6 \log N_0 + 1235$, $r^2 = 0.997$ for the modified logistic and Gompertz equations respectively. The
215 gradients were 16% and 33% greater for the modified logistic and Gompertz respectively over that
216 observed. In both cases the plot was a curve rather than the observed linear relationship. The sum
217 of squares between the observed TTD and that calculated using the two equations was minimised

218 by regressing the growth rate and lag, this gave growth rates of 0.0107 and 0.0122 log₁₀ cfu/ml/min
219 with a lag of 17 and 31 mins, respectively, but the gradient of the calculated TTD/ log initial
220 inoculum plots were now equal to the observed (-108.5 log₁₀ cfu/ml/min). Hence there is a
221 discrepancy between the fit of the modified logistic and Gompertz equations with the interpretation
222 of the observed values.

223

224 Multiple growth curves were produced *in-silico* using the observed rate, lag and the known initial
225 inocula and MPD. The calculated log numbers were transformed to numbers per ml and plotted
226 against time. If the modified Gompertz equation was an adequate descriptor of the observed data
227 then congruent plots should be observed. However, as the initial inocula decreased the modelled
228 curves became shallower, i.e. they do not reflect the observed OD curves (note a calibrant which
229 transforms the number to an OD will result in the same conclusion). The analyses performed were
230 also carried out using the modified logistic equation, resulting in the same conclusion: the modified
231 logistic model cannot reproduce the congruent shapes of the observed OD curves shown in Figure
232 1.

233

234 3.3 FITTING THE THREE PHASE LINEAR MODEL TO OD DATA

235 The 3PLM (Eq. 3) was fitted to the TTD data by minimising the sum of squares between the
236 observed TTD and the modelled; initial values of $\mu = 0.0092$ and lag = 0 mins were used (note the
237 MPD and the log of the detection numbers are fixed values). The fit gave $\mu = 0.00922$ (95% CI:
238 0.00914 – 0.00930), and a lag = -8.89 mins (95% CI: -12.84 to - 4.93). A plot of the calculated
239 TTD against the initial inocula gave a regression fit of $TTD_{calc} = -108.5 \log N_0 + 965.6$, $r^2 = 1.00$, i.e.
240 the 3PLM reproduced the observed TTD data and (by definition) was a straight line fit.

241

242 Using the full form of the 3PLM, multiple growth curves were produced *in-silico* using the
243 calculated rate, lag and the known initial inocula and MPD. The calculated log numbers were
244 transformed to numbers per ml and plotted against time. In this case the 3PLM produced
245 congruent curves and reproduce the initial shape of the OD curves (data not shown); however,
246 since the model gives only exponential growth until MPD is reached, i.e. there is no slow down in
247 the rate of growth, the discrepancy between the shapes of the observed OD and calculated
248 numbers quickly increases. In this case the 'simple' is good enough to fit the TTD data but not
249 'enough' to model the full data.

250

251 3.4 FITTING OF THE BARANYI MODEL TO OD DATA

252 The Baranyi model cannot be used to explicitly obtain the TTD for a given set of parameters,
 253 although this can be easily solved numerically. To fit the Baranyi model to the observed TTD data,
 254 and obtain a growth rate and lag, the observed TTD was used as the independent variable and the
 255 model used to fit the difference between the size of the detection inoculum and the initial inoculum.
 256 The estimated growth rate was $0.00918 \log_{10} \text{ cfu/ml/min}$ (95% CI: $0.00910 - 0.00927$), with a lag of
 257 -17.3 mins (95% CI: $-21.8 \text{ to } -12.9$).

258
 259 The Baranyi model was also used to generate multiple growth curves *in-silico*, using a growth rate
 260 of $0.00922 \log_{10} \text{ cfu/ml/min}$, a lag of zero minutes along with the given MPD of 9.8 and the size of
 261 the known initial inocula. The time taken to reach the inoculum detection value of 8.9 for all the
 262 simulated growth curves was obtained numerically using a simple linear interpolation procedure. A
 263 plot of the log initial inoculum against the calculated TTD gave a straight line fit with a regression fit
 264 of $\text{TTD}_{\text{calc}} = -108.4 \log_{10} N_0 + 956.49$, $r^2 = 0.999$. The multiple growth curves obtained were
 265 congruent and have the desirable feature of a slow down in the rate of growth as MPD is
 266 approached unlike the 3PLM (Figure 3).

267

268 3.5 OD – BARANYI CALIBRATION CURVE

269 Above the background OD, the Baranyi model and the OD data are 1:1 up to the maximum OD,
 270 i.e. there is a unique OD for each cfu/ml. Past the maximum OD, in the cases studied here, there is
 271 a reduction in the OD with incubation time, whereas the model stays at a constant MPD. This is a
 272 failing of the model as it is a purely growth rather than a growth and decay model. The 1:1 nature
 273 of the relationship up to the maximum OD can be used to construct a calibration curve between the
 274 optical density at a given time and the number of microbes per ml predicted from the Baranyi
 275 model. To construct the calibration curve ten observed OD curves were chosen and a plot of the
 276 OD (up to a maximum of 0.85) against the equivalent calculated numbers for the observation time
 277 constructed. Simple linear regression was applied (Eq.s 6a and 6b), Figure 4.

278

$$279 \text{ OD} = 1.308 \times 10^{-10} (\text{No.}) + 0.0946, r^2 = 0.997 \quad (\text{Eq.6a})$$

280

$$281 \text{ No.} = 7.625 \times 10^9 (\text{OD}) - 7.172 \times 10^8, r^2 = 0.997 \quad (\text{Eq.6b})$$

282

283 Where No. are the calculated microbial numbers per ml. Data up to an OD = 0.85 gave a good
284 linear relationship between OD and the calculated cfu/ml; at OD greater than 0.8, the inclusion of
285 the cubic and quadratic terms ($\text{No.} = -8.38 \times 10^9 (\text{OD})^3 + 1.23 \times 10^{10} (\text{OD})^2 + 2.67 \times 10^9 (\text{OD}) - 7.049 \times 10^8$,
286 $R^2 = 0.999$, $r^2 = 0.997$; $\text{OD} = 3.217 \times 10^{-30} (\text{No.})^3 - 2.787 \times 10^{-20} (\text{No.})^2 + 1.896 \times 10^{-10} (\text{No.}) + 0.0831$, R^2
287 $= 0.998$) gave better fits.

288

289 A calibration curve was also obtained from a regression analysis of plate counts against optical
290 density in the Bioscreen and gave a fit of $\text{OD} = 0.997 \times 10^{-10} (\text{No.}) + 0.14$, $r^2 = 0.956$.

291

292 Using the calibration curve derived from the Baranyi-analysis, the calculated microbial numbers
293 were converted to OD values. Figure 5 shows a direct comparison of the predicted OD/time curves
294 with the observed for five selected cases.

295

296 **3.6 CLASSICAL POPULATION LOGISTIC MODEL**

297 Fitting the classical logistic model (Eq. 5a) to the TTD data gave a straight line fit of $\text{TTD}_{\text{calc}} = -$
298 $105.43 \log_{10} N_0 + 943.59$, equating to a growth rate of $0.0095 \log_{10} \text{cfu/ml/min}$ (95% CI: $0.00945 -$
299 0.00955). The addition of a constant lag (Eq. 5b) improved the fit giving a straight line fit of TTD_{calc}
300 $= -108.48 \log_{10} N_0 + 956.56$, equating to a growth rate of $0.00923 \log_{10} \text{cfu/ml/min}$ (95% CI: 0.00915
301 $- 0.00932$). A lag of -14.3 minutes (95% CI: -18.4 to -10.2) was obtained; the correlation between
302 lag and growth rate was 0.90 , a result very similar to the fitting of the Baranyi equation.

303

304 **3.7 GROWTH RATE OF L. MONOCYTOGENES AT 30°C FROM OD DATA**

305 The TTD from a ten-fold dilution series of an initial standardised inoculum of *L. monocytogenes*
306 incubated at 30°C in TSB were obtained. A regression fit gave $\text{TTD} = -127.09 \log_{10} N_0 + 1121.8$, r^2
307 $= 0.999$; giving a growth rate of $0.00787 \log_{10} \text{cfu/ml/min}$. The intercept of $8.83 \log_{10} \text{cfu/ml}$ (95%
308 CI: $8.80 - 8.85$) suggests the absence of a lag. Initially the Baranyi model was fitted to the TTD
309 data using an MPD of 9.8 and a detection inoculum of 8.9 . The specific growth rate obtained was
310 $0.00786 \log_{10} \text{cfu/ml/min}$ (95% CI: $0.00780 - 0.00792$) and a lag of -17.5 mins (-22.5 to -12.5
311 mins). Using the calibration curve found previously (Eq.5a) the calculated numbers were
312 transformed to OD values. An MPD of 9.8 was found, however, to be too low for the maximum OD
313 observed. The MPD was increased to 9.9 and this gave reproducible OD curves. Changing the
314 MPD left the specific growth rate unchanged but the lag increased to -1.0 min.

315

316 **3.8 EFFECT OF PH**

317 An initial \log_{10} inoculum of 5.4 (determined from plate counts) was used to study the effect of a
318 range of pH (7.05 to 3.46) on growth. No visible growth was observed during the 3 day incubation
319 at 30°C at pH 4.42 or less. As the pH was reduced, the OD maximum was reduced and the rate of
320 change of OD also decreased. An analysis of the numbers per ml at an OD = 0.2 at pH 5.03, 4.95,
321 4.88 and 4.68 gave an average of 8.8 \log_{10} cfu/ml. There was no statistical difference between the
322 numbers obtained at the lower pH at OD = 0.2 and at the more optimal pH values. The OD data at
323 pH 6.95 were fitted with the Baranyi equation in concert with the calibration equation. Although the
324 initial log inoculum size was determined as 5.4 from plate counts, from the TTD/log initial inoculum
325 calibration curve obtained at 30°C a count of 5.5 was expected. The initial log cfu/ml was held at
326 5.5 and the specific growth rate, lag and the maximum population density were obtained by
327 regressing the calculated OD against the observed, Figure 6 displays these results. [Table 2](#) gives
328 the parameters obtained; in no case was a significant value for a lag observed (i.e., in all cases the
329 confidence interval for the calculated lags included zero).

330

331 4 Discussion

332 [Cuppers and Smelt \(1993\)](#) described an observed linear relationship between the log of the initial
 333 inoculum size and the time taken for the incubating culture to reach a specified turbidometric
 334 detection level due to a $10^{6.4}$ cfu/ml culture. They modeled the TTD data using a model based on
 335 the presence of a lag and the time taken for the initial culture to grow to the threshold value. Hence
 336 the growth rate could be calculated. Essentially this study modeled the underlying growth curve as
 337 a 3-phase linear model, ignoring the MPD value.

338

339 From the classic logistic equation, the time taken (t_N) to reach a specific population level (N) from a
 340 given initial value (N_0) is given by

341

$$342 \quad t_N = -\frac{1}{\mu} \ln N_0 + \frac{1}{\mu} \ln \left(\frac{N(M - N_0)}{M - N} \right) \quad (\text{Eq. 6})$$

343

344 where μ is the growth rate and M is the maximum population density (also known as the carrying
 345 capacity).

345

346 This is almost in the linear form $y = mx + c$, especially when $M \gg N_0$, and a plot of the time to the
 347 specific level against the natural log of the initial population number gives a gradient from which the
 348 growth rate can be found. When $N_0 = 1$, the intercept is obtained – the time taken for one organism
 349 to reach the specified detection number. One important point is that the logistic model as applied
 350 here has no lag. When we consider the phenomenon of microbial lag, we could simply state that if
 351 $t < t(\text{lag})$ then $N(t) = N(0)$ and change the time function to $t-t(\text{lag})$ to account for the change.

352 Physically this makes sense; the logistic equation is devoid of a lag, microbial lag is caused by an
 353 event (or sequence of events) before the onset of growth, hence is not part of the original
 354 derivation. Mathematically, however, the resulting logistic with lag equation has some undesirable
 355 features: the formula is discontinuous at the end of lag. This was, essentially, the equation reported
 356 by Jason (1983) and indeed the linear relationship between the log of the initial inocula (of *E. coli*
 357 growth measured using conductivity) and the time to reach a specific value was reported then.

358

359 The Baranyi model (Baranyi et al. 1993, 1993b) can be considered as a well-designed solution to
 360 the problem with the application of the Jason model. By invoking a time delay function, based on a
 361 biological foundation, the model becomes continuous, and remains biologically interpretable. A

362 major feature of the model has been the assignment of the so-called pre-exponential factor which
363 relates the fitness of an organism to thrive in an environment relative to another. If there is no
364 difference between environments then the theory states that there should be no lag if the organism
365 is transferred from one to the other and therefore the basic logistic model should apply – which is
366 the default for the Baranyi model.

367
368 The TTD data produced using the multiple inocula technique described could be well fitted using
369 the 3-PLM, the Baranyi and the logistic (with or without lag), the parameters obtained were
370 consistent between models and reflected the observed gradients well. Further, using a simple
371 conversion between OD and numbers (cfu/ml), the basic features of the OD/time plots could be
372 reproduced with these models. The rescaling functions (Eqs. 6a and 5b) overcome the peculiar
373 problem described by Baranyi and Roberts (1995): that direct fitting of viable count data to turbidity
374 or conductivity data or vice-versa should not be considered without additional information being
375 available. The calibration curves used in this work can be used since they are obtained indirectly
376 from pre-knowledge of the initial inoculum size, the maximum population density and the maximum
377 specific growth rate.

378
379 The modified logistic and modified Gompertz equations, however, failed to fit the observed data
380 and could not reproduce the observed OD/time plots. A simple simulation of growth data with a
381 given μ_{max} , lag and MPD for a number of initial inocula was produced using the modified Gompertz
382 (or indeed the modified logistic) equation. A plot of the initial log inocula against the TTD (Eq. 2) for
383 a given detection number ($\log N_d$) gave approximate straight line fits. The gradients of the line,
384 however, were not the reciprocal of the growth rates used. When TTD were obtained for the same
385 initial conditions, but for differing $\log N_d$ then these plots did not have the same gradient as was
386 observed, and as $\log N_d$ approached the MPD the plot became increasingly curved. From a casual
387 glance at equation 2, this equation cannot give a simple linear fit with respect to the initial log
388 inoculum used.

389
390 The 3PLM, the Baranyi and the classical population logistic model were the only models examined
391 which were capable of reproducing the straight line fit observed for the plot of the initial log
392 numbers against the TTD. The 3PLM, however, suffers from the inability to approach the MPD
393 continuously, and although giving the correct TTD for OD = 0.2 for the cultures, it failed to give the
394 approach to the maximum OD observed. The Baranyi and the classical logistic models did not
395 have this problem.

396

397 Applying the method of fitting the Baranyi model directly to another set of data (30°C), by simply
398 changing the MPD slightly, a good fit to the OD data was found. Equally, the lack of an apparent
399 lag (either from the fit of the model or from an analysis of the OD/time plot for large initial inocula),
400 suggested that the basic population logistic model would give an equivalent fit. This was indeed
401 found to be the case.

402

403 Several reports have suggested that the OD technique is limited as it requires high initial inocula
404 ([Baty et al. 2002](#); [Dalgaard et al. 1994](#); [Dalgaard and Koutsoumanis 2001](#); [Perni et al. 2005](#)). The
405 observed data described herein show that this assumption is not valid. If the growth rate of an
406 organism under ideal conditions is obtained using the multiple inoculum dilution method then any
407 subsequent study using non-ideal conditions can use a positive control to set the modelled fit. For
408 example in the study of pH, the growth rate at the ideal growth pH was known. The size of the
409 initial inoculum used could then be either found from the calibration curve (knowledge of the TTD)
410 or from plate counts (or both if confirmation was required). As conditions change (e.g. reducing pH)
411 the fixed parameters of the Baranyi model can be altered to fit the new growth rates and/or lag
412 induction. In the case studied here, the Baranyi model suggested that the growth rate reduced but
413 that lag was not induced over the pH range studied.

414

415 In 2002, McKellar *et al.* produced a study of the effect of pH on the growth of *Listeria*
416 *monocytogenes* (using the strain Scott A) stating that pH had no affect on the initial physiological
417 state. A graph of the initial log inoculum (per well) against the TTD for a range of pH showed
418 multiple linear slopes apparently intercepting the \log_e inoculum axis at 20.086 ± 1.092 : equivalent
419 to a range of 8.25 to 9.2 \log_{10} cfu per well. This range encompasses the 8.37 \log_{10} cfu/well
420 detection threshold found with this work. Further our study of the effect of pH suggests that there
421 was no change in lag— only a change in growth rate. The difference between our interpretation and
422 that of McKellar *et al.* is the presence or not of a lag. However, an important point must be made
423 with respect to the detection value used in [McKellar and Knight \(2000\)](#) and McKellar *et al.* 2002: if
424 the detection threshold is equivalent to 3.5×10^6 cfu/well, then all the TTD values of wells containing
425 greater than 3.5×10^6 cfu/well should be zero; from figure 4 of McKellar *et al.* 2002 this is clearly not
426 the case.

427

428 In [McKellar and Knight \(2000\)](#) the time of lag was calculated as the difference between observed
429 TTD data and the theoretical TTD plot of the log of the initial inoculum based on a detection limit of

430 3.5×10^6 cfu per Bioscreen well for a given growth rate. Observed data had the theoretical growth
431 rate but had greater TTD values since a lag was present. The observed data at pH 7.2 gave a
432 regression fit of $TTD_{30^\circ C} = -132.84 \log_{10} I_0 + 1221$, but was quoted in terms of cfu per well, which
433 were filled with 350 μ l of culture. The growth rate obtained was very similar to that obtained from
434 the data observed in this report (-127.09), but the intercept was higher than was found (in terms of
435 cfu/ml, the intercept was calculated to be 1281 mins, whereas a value of 1122 +/- 4.6 was observed
436 in this study). At lower pH, the growth rate reduces and according to McKellar *et al.* since the
437 physiological state is constant the lag increases and this can be obtained from the difference of the
438 observed to the theoretical intercept on the TTD axis. However, if this was the case then at the
439 lower pH values with reduced growth rates, according to the logistic model (eq. 6) a vertical
440 separation between the horizontal inoculum axis and the observed TTD should have been
441 observed and this does not appear to be the case.

442

443 We suggest the discrepancy between the work reported here and the interpretation of the
444 observations of these other workers may be due to an inadvertent use of the threshold detection
445 value vs. a TTD based on a specific OD. Figure 2 shows the TTD for different criteria: the OD
446 criteria of 0.09 is slightly above the background, this has a detection value of approximately 8×10^6
447 cfu/well (recalculated for a volume of 350 μ l per well). If this calibration curve was considered as the
448 threshold curve, then any of the other calibrants would have a constant time delay (i.e. interpreted
449 as lag) between them and this line. This may explain the difference in interpretation between the
450 studies. We suggest that the work of McKellar shows a constant lag over the pH range used.

451

452 From the interpretation of the Baranyi model (Baranyi *et al.* 1993b), the physiological state of the
453 cells, denoted as α_0 , at t_0 is a measure of the fitness of the cell in one environment to cope with
454 being placed in a new environment. The negative natural log of α_0 is the product of the maximum
455 specific growth rate and the lag. Hence, if there is no lag then $\ln(\alpha_0) = 0$. Both the study described
456 herein and we believe that of McKellar *et al.* suggest, however, that the automatic link of lag and
457 growth may be globally invalid; growth rates can alter without inducing lags (e.g. the observed data
458 on the change of pH). Conversely, lags can be induced without inducing changes in growth rate
459 (albeit after recovery from injury) as shown by the work of [Stephens et al.\(1997\)](#).

460

461 **4.1 CONCLUSIONS:**

462 We would simply conclude, therefore, that the Baranyi model is the most capable primary model of
463 those examined, but that the *modified* logistic and the *modified* Gompertz should not be used as
464 Primary models for TTD experiments since they cannot reproduce observed data.

465 **5 References**

466 Alexandrov, G. A., 2008. Forest growth in the light of the thermodynamic theory of ecological
467 systems. *Ecological Modelling* 216,102 – 106.

468

469 Baranyi, J., 1997. Simple is good as long as it is enough. *Food Microbiology* 14, 189-192.

470

471 Baranyi, J., Roberts T.A. and McClure, P., 1993. A non-autonomous differential equation to model
472 bacterial growth. *Food Microbiology* 10, 43-59.

473

474 Baranyi, J., Roberts, T.A. and McClure, P.J., 1993b. Some properties of a non-autonomous
475 deterministic growth model describing the adjustment of the bacterial population to a new
476 environment. *Journal of Mathematics Applied in Medicine and Biology* 10, 293-299.

477

478 Baranyi, J and Roberts, T.A., 1994. A dynamic approach to predicting bacterial growth in food
479 *International Journal of Food Microbiology* 23, 277-294.

480

481 Baranyi, J and Roberts, T.A., 1995. Mathematics of predictive food microbiology. *International*
482 *Journal of Food Microbiology* 26, 277-294.

483

484 Baty, F., Flandrois, J.P. and Delignette-Muller, M.L., 2002. Modeling the lag time of *Listeria*
485 *monocytogenes* from biable count enumeration and optical density data. *Applied and*
486 *Environmental Microbiology* 68, 5816-5825.

487

488 Bidlas, E., Du, T., and Lambert, R.J.W., 2008. An explanation for the effect of inoculum size on
489 MIC and the growth/no growth interface. *International Journal of Food Microbiology* 126, 140-152.

490

491 Buchanan, R.L., Whiting, R.C., and Damert, W.C., 1997. When is simple good enough: a
492 comparison of the Gompertz, Baranyi, and three-phase linear models for fitting bacterial growth
493 curves. *Food Microbiology* 14, 313-326.

494

495 Cuppers, H.G.A.M and Smelt, J.P.P.M., 1993. Time to turbidity measurements as a tool for
496 modelling spoilage by *Lactobacillus*. *Journal of Industrial Microbiology* 12, 168-171.

497

- 498 Dalgaard, P. and Koutsoumanis, K., 2001. Comparison of maximum specific growth rates and lag
499 times estimated from absorbance and viable count data by different mathematical models. Journal
500 of Microbiological Methods 43, 183-196.
- 501
502 Dalgaard, P., Ross, T., Kamperman, L., Neumeyer, K., McMeekin, T.A., 1994. Estimation of
503 bacterial growth rates from turbidometric and viable count data. International Journal of Food
504 Microbiology 23, 391-404
- 505
- 506 Garthright, W.E., 1997. The three phase linear model of bacterial growth: a response. Food
507 Microbiology 14, 193-195.
- 508
- 509 Jason, A.C., 1983. A deterministic model for monophasic growth of batch cultures of bacteria.
510 Antonie van Leeuwenhoek 49, 513-536.
- 511
- 512 Li, H., Xie, G., Edmundson, A., 2007. Evolution and limitations of primary mathematical models in
513 predictive microbiology. British Food Journal 109, 608 – 626.
- 514
- 515 McKellar, R.C., and Knight, K.P., 2000. A combined discrete-continuous model describing the lag
516 phase of *Listeria monocytogenes*. International Journal of Food Microbiology 54, 171 – 180.
- 517
- 518 McKellar, R.C., Lu, X., and Knight, K.P., 2002. Growth pH does not affect the initial physiological
519 state parameter (p_0) of *Listeria monocytogenes*. International Journal of Food Microbiology 73, 137
520 – 144.
- 521
- 522 Perni, S., Andrew, P.W., and Shama, G., 2005. Estimating the maximum growth rate from
523 microbial growth curves : definition is everything. Food Microbiology 22, 491 – 495.
- 524
- 525 Pruitt, K. M. and Kamau, D. N., 1993. Mathematical models of bacterial growth, inhibition and
526 death under combined stress conditions. Journal of Industrial Microbiology 12, 221-231.
- 527
- 528 Stephens, P.J., Joynson, J.A., Davies, K.W., Holbrook, R., Lappin-Scott, H.M. and Humphrey, T.J.,
529 1997. The use of automated growth analyser to measure recovery times of single heat injured
530 Salmonella cells. Journal of Applied Microbiology 83, 445-455.
- 531

532 Zwietering, M. H., Jongenburger, I., Rombouts, F. M. and van 't Riet, K.,1990. Modeling of the
533 bacterial growth curve. Applied and Environmental Microbiology 56, 1875-1881.
534

535 **6 Tables**

536

537 Table 1. Parameter estimates from linear regression fits to TTD data for multiple initial inocula of
 538 *Listeria monocytogenes* at 37°C in TSB for different time to detection criteria at 600nm.

OD criterion	Coefficient	Gradient		Coefficient	Intercept		r^2	log ID*
		Lower 95%	Upper 95%		Lower 95.0%	Upper 95.0%		
0.09	-104.17	-109.15	-99.19	766.52	740.22	792.81	0.981	7.358
0.1	-104.17	-105.83	-102.50	824.96	816.37	833.54	0.997	7.919
0.2	-108.49	-109.60	-107.38	956.29	950.29	962.30	0.999	8.814
0.3	-109.20	-110.14	-108.26	996.36	991.23	1001.48	0.999	9.124
0.4	-110.51	-111.54	-109.48	1032.31	1026.56	1038.05	0.999	9.341
0.5	-110.23	-111.31	-109.14	1056.05	1050.08	1062.03	0.999	9.581
0.6	-110.53	-111.63	-109.43	1085.84	1079.78	1091.90	0.998	9.824
0.7	-110.34	-111.75	-108.93	1113.02	1105.24	1120.79	0.997	10.09
0.8	-110.20	-112.44	-107.95	1153.58	1141.18	1165.97	0.994	10.47
0.9	-110.32	-113.38	-107.26	1216.46	1199.52	1233.41	0.988	11.03
0.95	-109.88	-113.23	-106.53	1252.31	1233.60	1271.02	0.987	11.40
1.0	-110.81	-114.12	-107.50	1285.19	1266.28	1304.10	0.993	11.60

539 *Log ID is the calculated intercept on the log lo axis for the given regression fit; the MPD (from
 540 plate counts) was 9.8 log cfu/ml.

541

542

543 Table 2. Parameter Estimates for the Baranyi equation fitting of OD data at various pH values at
 544 30°C

pH	Mu	LCL	UCL	MPD	-95% CI	+95% CI
6.95	0.01870	0.01864	0.01875	9.771	9.769	9.773
5.65	0.01630	0.01625	0.01636	9.778	9.776	9.781
5.51	0.01472	0.01467	0.01478	9.777	9.774	9.781
5.03	0.01333	0.01328	0.01338	9.780	9.776	9.784
4.95	0.00984	0.00980	0.00988	9.736	9.732	9.741
4.88	0.00812	0.00808	0.00816	9.643	9.639	9.647
4.68	0.00592	0.00591	0.00594	9.566	9.563	9.569

545 Growth rate as ln cfu/ml/min

546 7 Figures Captions

547

548 Figure 1. Optical density-incubation time plot for the growth of multiple initial inocula of *Listeria*
549 *monocytogenes* (isolate Lm252) at 37°C in TSB. Each curve represents a single initial inoculum
550 ranging from 9.1 log₁₀ cfu/ml to 1 cfu/ml (left to right), wells with no cells present failed to show
551 growth (horizontal OD at background level).

552

553 Figure 2. The time to detection of multiple initial inocula of *Listeria monocytogenes* at 37°C in TSB.
554 The TTD criterion was set at OD =0.09 (▲), 0.1 (□), 0.2 (■), 0.4 (○), 0.6 (●). An OD = 0.2 at
555 600nm was equal to 8.81 log₁₀ cfu/ml.

556

557 Figure 3. Predicted microbial numbers of *L. monocytogenes* (Lm252) with time from the Baranyi
558 model, with parameters $\mu=0.00921$, Lag = -8.88 mins, MPD = 9.8 log₁₀ cfu/ml, with a range of initial
559 inocula.

560

561 Figure 4. Plot of the observed OD against the calculated numbers/ml from the associated Baranyi
562 equation (diamonds), the solid line is the regression fit used in this study. The calibration curve
563 obtained from plate counts (squares) is also displayed.

564

565 Figure 5. Comparison of the observed optical density incubation time plot (symbols) and the
566 calculated (solid lines) for *Listeria monocytogenes* incubated at 37°C with initial log₁₀ inocula of
567 (from left to right) 8.789, 7.789, 6.585, 5.09, and 3.284 respectively.

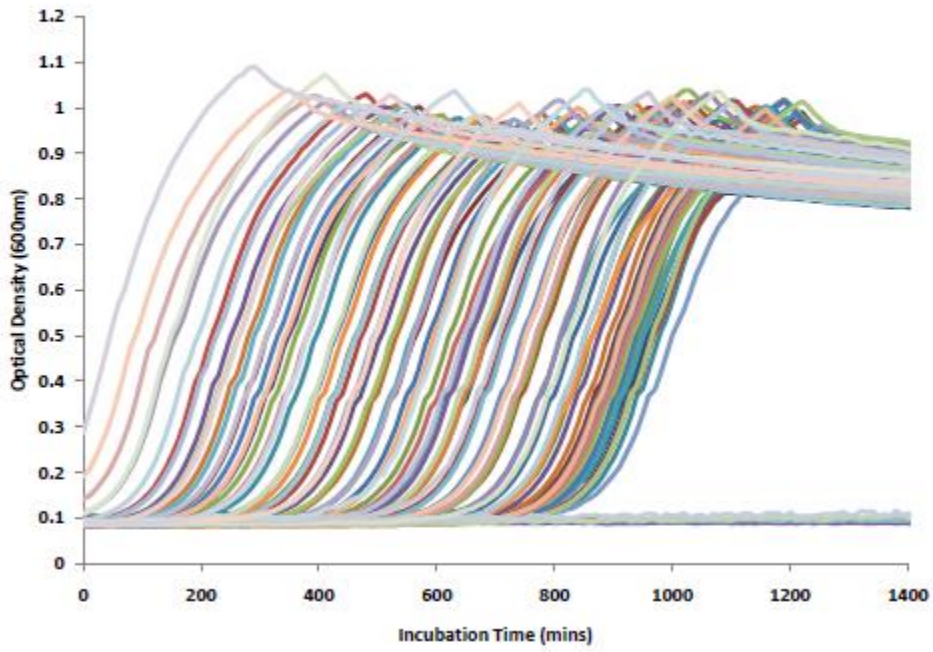
568

569 Figure 6. Comparison of the observed optical density incubation time plot (symbols) and the
570 calculated (solid lines) for *Listeria monocytogenes* incubated at 30°C with initial inocula of 4.97
571 log₁₀ cfu/ml, at pH 6.95, 5.65, 5.51, 5.03, 4.95, 4.88, 4.68 from left to right respectively, pH 4.42
572 failed to show any visible growth during the period of incubation (constant OD = 0.088).

573

574

Figure 1.

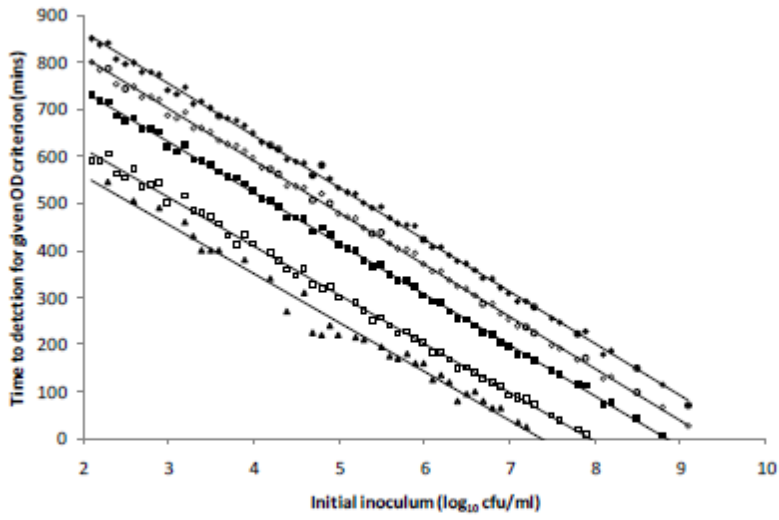


575

576

577 Figure 2

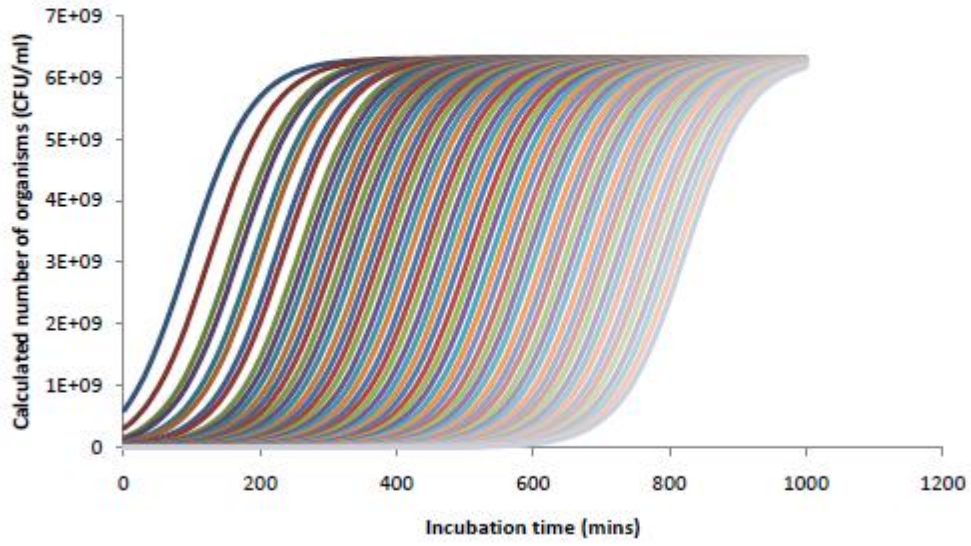
578



579

580

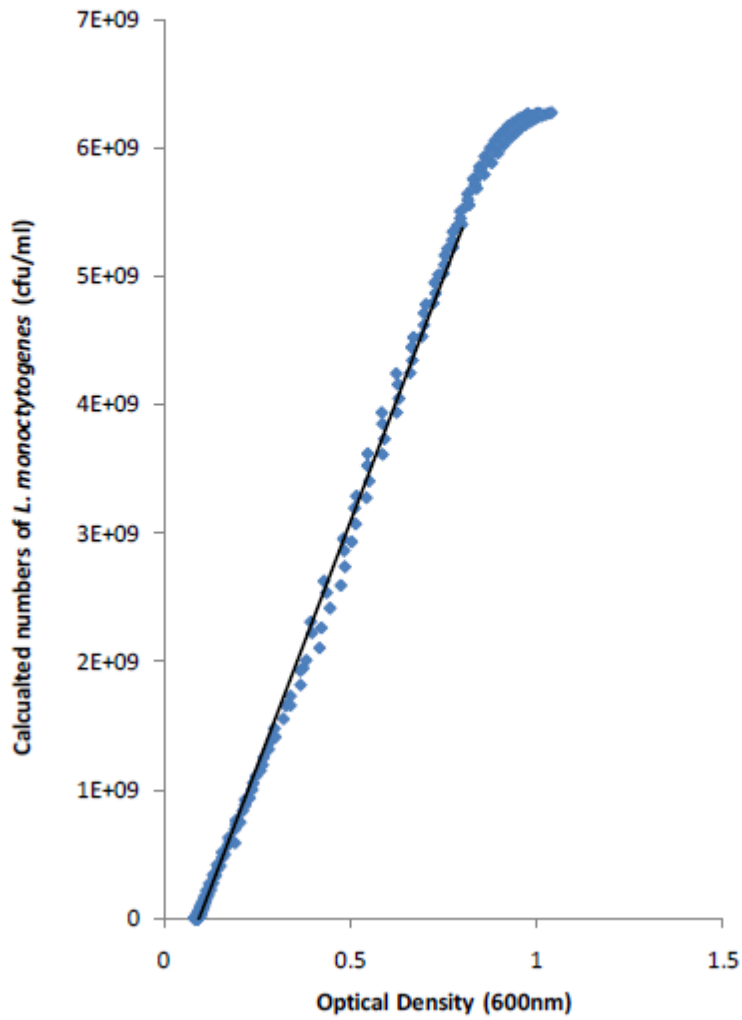
Figure 3



581

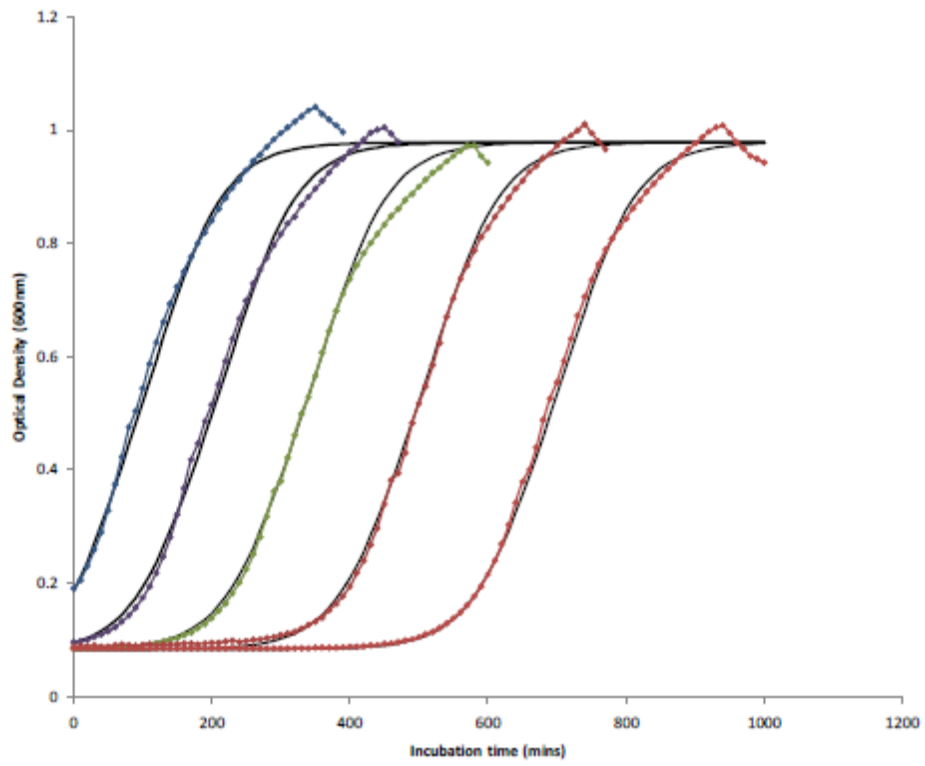
582

Figure 4



583
584

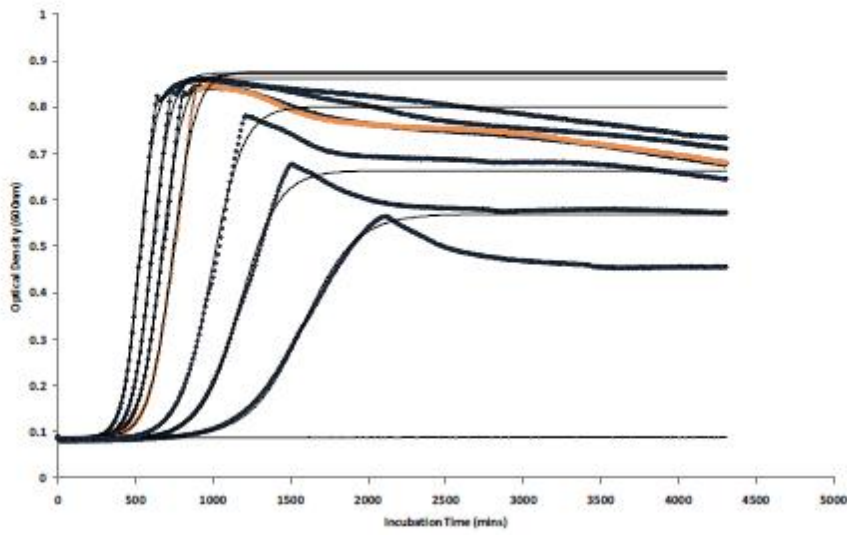
Figure 5



585

586

Figure 6



587

Growth curve prediction from optical density data

Mytilinaios, Ioannis

2012-03-15T00:00:00Z

I Mytilinaios, M. Salih, H.K. Schofield and R.J.W. Lambert. Growth curve prediction from optical density data. *International Journal of Food Microbiology*, Volume 154, Issue 3, 15 March 2012, Pages 169-176.

<http://dx.doi.org/10.1016/j.ijfoodmicro.2011.12.035>

Downloaded from CERES Research Repository, Cranfield University